Osmotic Effects on the Electrical Properties of Arabidopsis Root Hair Vacuoles in Situ[1]

Roger R. Lew*

Biology Department, York University, Toronto, Ontario M3J 1P3, Canada

To assess the role of the vacuole in responses to hyperosmotic and hypo-osmotic stress, the electrical properties of the vacuole were measured in situ. A double-barrel micropipette was inserted into the vacuole for voltage clamping. A second double-barrel micropipette was inserted into the cytoplasm to provide a virtual ground that separated the electrical properties of the vacuole from those of the plasma membrane. Osmotic stress causes immediate electrical responses at the plasma membrane (Lew RR [1996] Plant Physiol 97: 2002–2005) and ion flux changes and turgor recovery (Shabala SN, Lew RR [2002] 129: 290–299) in Arabidopsis root cells. In situ, the vacuole also responds rapidly to changes in extracellular osmotic potential. Hyperosmotic treatment caused a very large increase in the ionic conductance of the vacuole. Hypo-osmotic treatment did not affect the vacuolar conductance. In either case, the vacuolar electrical potential was unchanged. Taken in concert with previous studies of changes at the plasma membrane, these results demonstrate a highly coordinated system in which the vacuole and plasma membrane are primed to respond immediately to hyperosmotic stress before changes in gene expression.

Osmotic stresses, caused by drought or excess water (hyperosmotic and hypo-osmotic stresses, respectively), are a constant challenge for higher plants. At extremes, the outcome can be plant death. In the context of agricultural needs, many crop lands are marginal with respect to water availability. Therefore, it is not surprising that plant responses to osmotic stresses are a major area of plant research. Adaptation to stress and the signal transduction mechanisms that trigger osmoresponses are two areas in which there have been major accomplishments recently (Zhu, 2002). Many of the recent advances have been in the identification of the genes responsible for various aspects of transduction and response. Because of gene homologies, osmoresponses in yeast have offered many insights for plant physiologists (Hasegawa et al., 2000; Zhu, 2002; Meijer and Munnik, 2003). However, it is also very clear that the multicellular complexity of plants, and especially the adaptability associated with zones of expansion, play a key role in the long-term survival of the plant (Ober and Sharp, 2003). In Arabidopsis, it has been established that one of the immediate effects of osmotic stress, hyperosmotic or hypo-osmotic, is the change in the electrical properties of the plasma membrane (Lew, 1999). These changes occur within 1 min, whereas expression of AtMEKK1, a component of a mitogen-activated protein kinase cascade responsible for activating osmoresponses, occurs within about 5 min (Covic et al., 1999). In the case of hyperosmotic shock, these rapid changes are followed by turgor recovery, a process that takes about 30 min to complete, and is caused by large changes in the net ion fluxes across the plasma membrane (Shabala and Lew, 2002). A major aspect of osmoregulation and turgor recovery must involve coordinated changes in vacuole and plasma membrane ion fluxes. The role of the vacuole in turgor regulation has long been recognized (Matile, 1978), and many vacuolar transporters have been identified (Barkla and Pantoja, 1996; Martinoia et al., 2000; Maeshima, 2001), including aquaporins that maximize water movement and therefore minimize changes to cytoplasmic volume (Tyerman et al., 1999). To determine the role of the vacuole in rapid osmosensing and response, the vacuolar potential and vacuolar conductance (G_v) were measured in situ. This required dual impalements with double-barrel micropipettes, one into the cytoplasm, the other into the vacuole.

RESULTS

Measurements of Vacuolar Electrical Properties

Growing root hairs that were in medial or near medial optical section were impaled after they had grown to a length of 80 to 100 μm (Fig. 1). At this time, the apex was still cytoplasm-rich, making impalement into the cytoplasm unambiguous. The nuclei had migrated into the hair, creating a region at the base of the root hair that was highly vacuolated. The vacuole was impaled in this region. After the impalements, there was no indication of cellular damage: cytological structure was undisturbed (Fig. 1). An experimental example of electrical measurements is shown in Figure 2. Initially, the cytoplasm

[1] This work was supported by the Natural Sciences and Engineering Research Council of Canada (Discovery Grant).

* Corresponding author; e-mail planters@yorku.ca; fax 416–736–5698.

Article, publication date, and citation information can be found at www.plantphysiol.org/cgi/doi/10.1104/pp.103.031427.

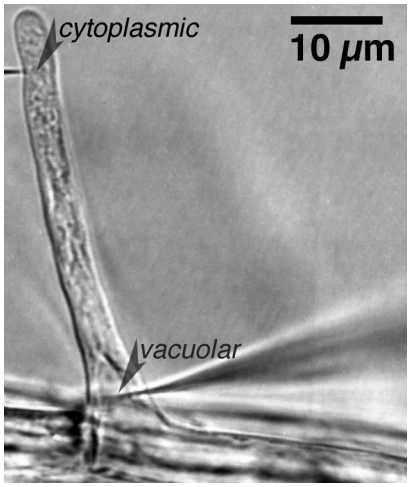

Figure 1. Example of cytoplasmic and vacuolar impalements into a growing root hair. First, the cytoplasm-rich tip of the hair was impaled with a double-barrel micropipette. The second double-barrel micropipette was impaled at the base of the hair into a vacuolar-rich zone. At this stage of root hair development, the nucleus has migrated from the base of the hair into the hair, and is about 5 μm above the vacuole impalement in this example.

was impaled near the root hair tip, followed by impalement into the vacuolar-rich region at the base of the hair. Preliminary experiments using injection of fluorescent dyes (Lew, 2000) indicated that for the cytoplasm impalement, the micropipette tip was located in the cytoplasm. For vacuolar impalements, occasional examples in which the vacuole did not fill with fluorescent dye were observed (data not shown). Instead, the fluorescence "wrapped around"

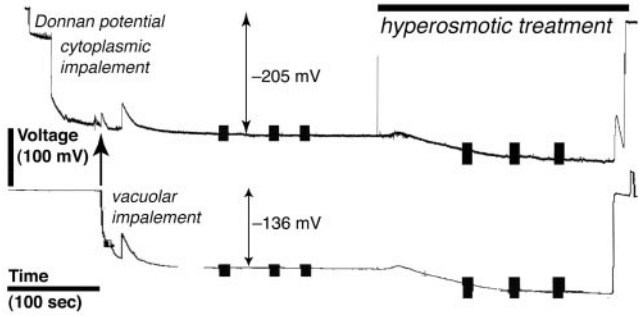

Figure 2. Example of an electrical measurement. The electrical potential of the cytoplasmic impalement is shown in the upper trace and the vacuolar impalement is shown in the lower trace. In the recording for the cytoplasmic potential, the micropipette tip "reports" the cell wall (Donnan) potential before entry into the cytoplasm. A transient depolarization occurred when the vacuole was impaled (arrow), and when the micropipette was removed from the vacuole. Note that the vacuolar impalement (vacuole to outside, E_{vo}) measures the E_m and E_v in series. E_{vo} is the sum of the E_m and E_v (E_v, +69 mV in this example). Vertical bars represent current-voltage measurements. Hyperosmotic treatment (as marked) was APW7 plus 50 mM mannitol and 50 mM sorbitol. Note that both traces hyperpolarized. The hyperpolarization seen in the vacuolar impalement is because the micropipette measures the vacuole and plasma membrane in series, shown schematically in Figure 3.

the micropipette tip and entered the cytoplasm, suggesting that the flexible vacuolar membrane was not punctured by the micropipette tip. It was possible to establish the vacuolar location of the micropipette tip in electrical measurements because voltage clamping failed when both double-barrel micropipette tips were located in the cytoplasm. This occurred at a significant frequency (aborted experiments were not tabulated, but were about 70% of all measurements). In the experimental example (Fig. 2), having established the correct location of the micropipette tips using voltage clamp, the culture dish was perfused with APW7 plus 50 mM sorbitol and 50 mM mannitol. Both micropipette tips registered a hyperpolarization. This is because the vacuolar electrodes measure the vacuolar membrane potential (E_v) and plasma membrane potential (E_m) in series (Fig. 3A). Thus, the

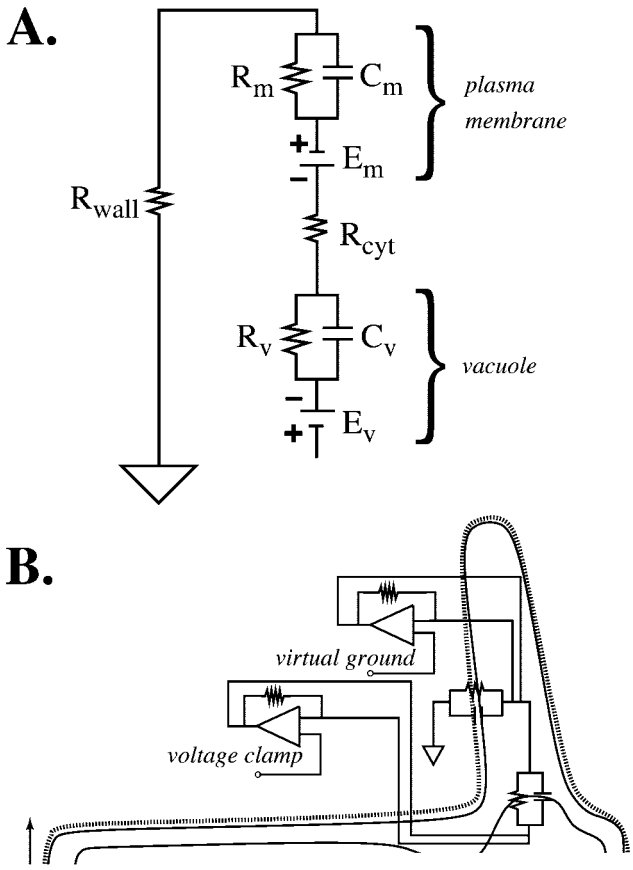

Figure 3. Electrical description of a root hair and the measurement technique. A, Electrical network of a plant cell. The symbols have their usual meanings (Horowitz and Hill, 1989). R_m and R_v are the resistances of the plasma membrane and vacuole, respectively. C_m and C_v are the capacitances. An impalement into the vacuole will measure the vacuolar and plasma membrane electrical properties in series. B, Electrical schematic of root hair electrical measurements. To isolate the vacuole electrical properties from the electrical properties of the plasma membrane, voltage clamping was performed through a double-barrel micropipette impaled into the vacuole, while the cytoplasm was held at virtual ground, relative to the vacuole.

hyperpolarization of the plasma membrane (Lew, 1996) would be measured by the micropipette located in the vacuole. The E_v could be calculated by subtracting the potential measured in the vacuole from the potential measured in the cytoplasm. To isolate the vacuole's current-voltage relations from those of the plasma membrane, it was necessary to hold the cytoplasm at a constant potential. This was done by configuring the voltage clamping apparatus as a "virtual ground" (Fig. 3B), maintaining the plasma E_m at the resting potential measured just before the voltage clamp.

Hyperosmotic Treatment

In Arabidopsis root hairs growing in APW7, treatment with osmoticum (APW 7 plus 50 mM sorbitol and 50 mM mannitol) is reported to cause hyperpolarization of the plasma E_m by about −25 mV from an initial potential of about −190 mV (Lew, 1996) and a decrease in conductance from 190 to 167 nanoSiemens (nS; Lew, 1996). A similar hyperpolarization was observed in the present work (an example is shown in Fig. 4). The initial potential of −170 ± 18 mV (n = 8) hyperpolarized −33 ± 16 mV to −203 ± 26 mV. The E_v relative to the cytoplasm was essentially unchanged by hyperosmotic treatment. Before, it was 22 ± 22 mV (n = 8; range of 4–69 mV). After hyperosmotic treatment, it was 24 ± 20 mV (range of 2–65 mV; Fig. 5). In contrast to the decrease in conductance observed for the plasma membrane (Lew, 1996), the G_v increased from 637 ± 144 nS to 1,412 ± 1,046 nS (n = 6; the increase in G_v ranged from 17 to 2,223 nS; Table I). The increase was statistically significant (Fig. 6).

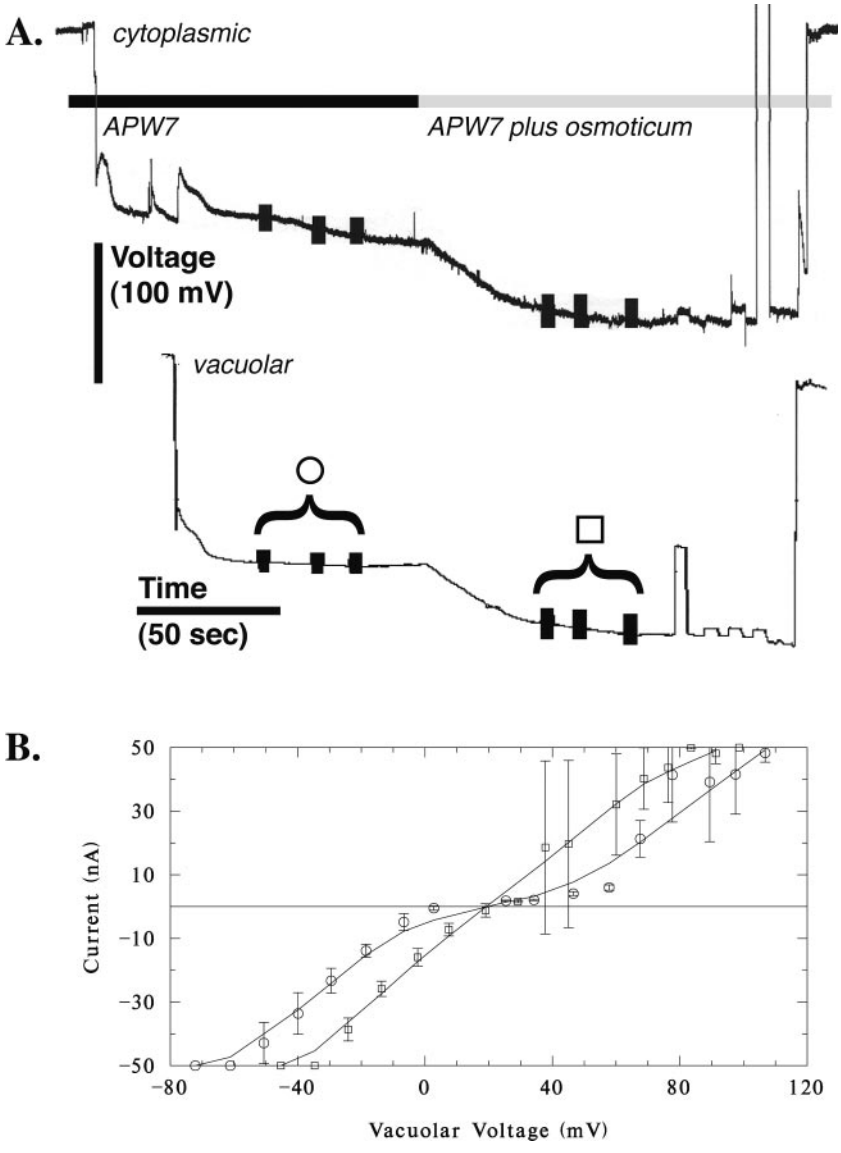

Figure 4. Vacuolar current-voltage relations: hyperosmotic effect. A, An example of potential measurements from the cytoplasm and vacuole. Vertical bars on the potential traces show when voltage clamping was performed to obtain the current-voltage relation. B, Current-voltage measurements before (circles) and after (squares) hyperosmotic treatment. The data are mean ± SD of three measurements, as shown in A. High SDs at positive voltages are due to a progressive increase in current during the measurements after hyperosmotic treatment. For all experiments, most of the current-voltage relations exhibited voltage-activated currents at negative and positive voltages (four of six experiments), or were linear. There was no systematic relation between the shape of the current-voltage curves and treatment (before and after).

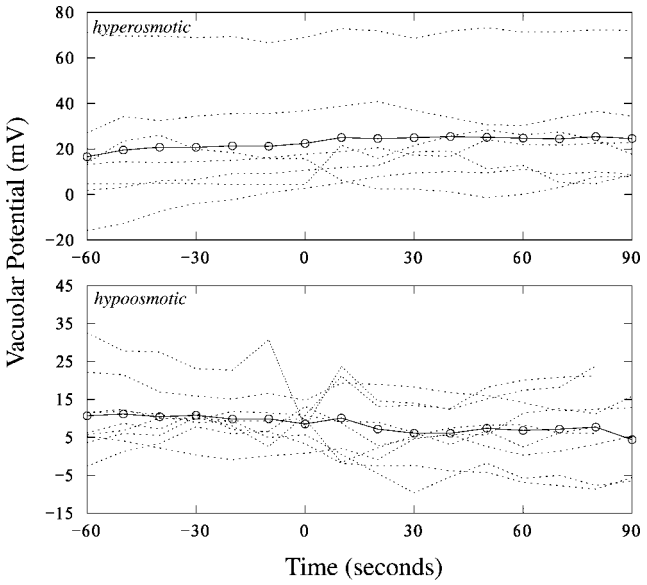

Figure 5. Vacuolar potentials before and after hyperosmotic (top) and hypo-osmotic (bottom) treatments. Individual experiments (dotted lines) are shown along with averages (circles and solid lines). Treatments began at 0 s.

Hypo-Osmotic Treatment

Root hairs growing in APW7 containing 50 mM sorbitol and 50 mM mannitol were treated to hypo-osmotic shock by changing the solution to APW7 alone. An experimental example is shown in Figure 7. Hypo-osmotic shock is known to cause depolarization of the E_m by about 40 mV from an initial potential of about −190 mV (Lew, 1996) and an increase in G_v from 153 to 177 nS (Lew, 1996). A similar depolarization was observed in the present work. The initial potential of −160 ± 20 mV (n = 9) depolarized 27 ± 19 mV to −132 ± 35 mV. In the growing root hairs adapted to APW7 plus osmoticum, the vacuole potential was lower than root hairs growing in APW7 (11 mV compared with 22 mV), but not significantly so (independent t test, $P > 0.15$). The E_v was essentially unchanged by hypo-osmotic treatment. Before, it was 11 ± 6 mV (n = 9; range of 2–23 mV) relative to the cytoplasm. After hypo-osmotic treatment, it was 8 ± 9 mV (range of −8 to 21 mV; Fig. 5). In contrast to the increase in G_v observed for the plasma membrane (Lew, 1996), the G_v was unchanged: 541 ± 219 nS before and 600 ± 298 nS (n = 8) after hypo-osmotic treatment (Table I; Fig. 6; the G_v in five of eight experiments declined and increased in three of eight experiments; the change in G_v ranged from a decline of 58 nS to an increase of 342 nS).

DISCUSSION

The major compartments of a higher plant cell are the vacuole and the cytoplasm, but the vacuole dominates due to its large volume compared with the cytoplasm. In the context of osmotic adjustments required for regulation of root cell turgor (Shabala and Lew, 2002), the vacuole must play an important role, based solely upon its volume. Osmotically active ions are found at similar concentrations in the cytoplasmic and vacuolar compartments. In fresh water algae, reported cytoplasmic concentrations (in mM) are K^+ (100), Na^+ (20), and Cl^- (45) compared with vacuolar concentrations of K^+ (70), Na^+ (40), and Cl^- (130), whereas in higher plants, cytoplasmic concentrations (in mM) are K^+ (140), Na^+ (40), and Cl^- (45) and vacuolar concentrations are K^+ (105), Na^+ (30), and C^- (100). These values are averages of data compiled by Luttge and Higinbotham (1979). Using triple-ion, pH, and potential-measuring electrodes (Felle, 1994; Miller et al., 2001), it is known that vacuolar and cytoplasmic [K^+] varies in response to changes in K^+ supply (Walker et al., 1996), cell type, and salt stress (Cuin et al., 2003). Because the vacuole must remain at the same osmotic potential as the cytoplasm (to avoid turgor-driven volume changes), osmoregulation must occur between the two compartments, which would require changes in ion concentration.

Unfortunately, due to its location within the cell, the vacuole is difficult to access in situ for measurements of ion flux and other aspects of transport physiology except when giant cells are used, such as Characeae algae (e.g. Shimmen and Nishikawa, 1988)

Table I. *Summary of electrical changes at the plasma membrane (E_m) and the vacuolar membrane (E_v and G_v)*

Treatment	E_m	E_v	G_v
	mV		*ns*
Hyperosmotic treatment			
APW7	−170 ± 18 (n = 8)	22 ± 22 (n = 8)	637 ± 144 (n = 6)
APW7 plus osmoticum	−203 ± 26	24 ± 20	1,412 ± 1,046
Change	−33.5 ± 15.5	1.6 ± 8.6	776 ± 919
(range)	*(−56–−4)*	*(−12–14)*	*(17–2,223)*
Hypoosmotic treatment			
APW7 plus osmoticum	−160 ± 20 (n = 9)	11 ± 6 (n = 9)	541 ± 219 (n = 8)
APW7	−132 ± 35	8 ± 9	600 ± 298
Change	+27 ± 19	−2.4 ± 8.5	59 ± 149
(range)	*(4–55)*	*(−19–7)*	*(−58–542)*

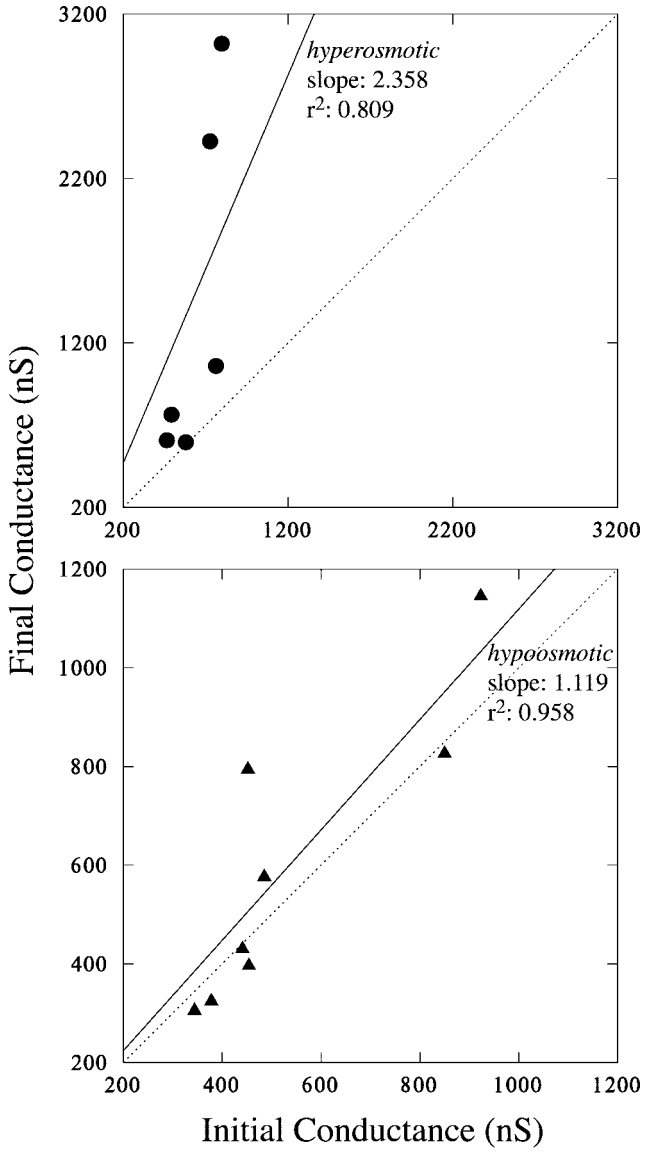

Figure 6. G_v changes. Final G_v is plotted versus initial G_v. Linear regression ($y = bx$) was performed to evaluate changes caused by hyperosmotic (top) or hypo-osmotic (bottom) treatments. The dotted diagonals show the expected relation if no change in G_v occurred (a slope of 1). For hyperosmotic treatment, G_v increased in all experiments. The increase was 2.36 ± 0.51 (slope ± SE; $P = 0.006$). Even if the two largest G_v increases are removed from the dataset, the G_v increase (1.32 ± 0.10) is still highly significant ($r^2 = 0.982$, $P = 0.001$). For hypo-osmotic treatment, most data clustered about the diagonal, below or above, the slope was 1.12 ± 0.09 ($P < 10^{-3}$).

and the marine alga *Valonia utriculatus* (Heidecker et al., 2003). This means that the vast majority of research has used isolated vacuoles removed from their in situ environment. Considerable attention has been paid to the role of vacuolar ion transport in guard cells. Stomatal opening and closing is a turgor-active process that involves coordination of vacuolar and plasma membrane ion transport (Schulz-Lessdorf et al., 1994). Vacuolar ion channels have been characterized on the basis of time dependence of voltage activation (slow-activating and fast-activating nonselective cation channels; Barkla and Pantoja, 1996) and ion selectivity (Ca^{2+}-selective channels [White, 2000] and Cl^- channels [Pei et al., 1996]). Modulators of vacuolar ion channels include not only calcium (Hedrich and Neher, 1987; Reifarth et al., 1994; Ward and Schroeder, 1994), but also calmodulin (Bethke and Jones, 1994), calcineurin (Allen and Sanders, 1995), inositol 1,4,5-trisphosphate (Alexandre and Lassalles, 1990), Ca^{2+}-dependent protein kinase-activated Cl^- channel (Pei et al., 1996), Mg^{2+} (Pei et al., 1999; Carpaneto et al., 2001), K^+ (Pottosin and Martinez-Estevez, 2003), 14-3-3 proteins (van den Wijngaard et al., 2001), polyamines (Dobrovinskaya et al., 1999; Bruggemann et al., 1998), reductive agents (Carpaneto et al., 1999), pH (Berecki et al., 2001), and acetylcholine (Gong and Bisson, 2002). Most notable in the context of osmotic effects is a report of a nonspecific (relative permeability ratio [P_K/P_{Cl}] of approximately 3) ion channel activated by hydrostatic pressure or an osmotic gradient (Alexandre and Lassalles, 1991). In all cases, the effect of the modulators was examined using isolated vacuoles. However, how does the vacuole respond in situ? The experiments reported here are an initial characterization of in situ G_v changes in response to osmotic stress.

Considerable information is available on plasma membrane ion transport in root hairs (Lew, 1991; Bouteau et al., 1999; Ivashikina et al., 2001). To isolate the vacuolar electrical properties from those of the plasma membrane required the use of a virtual ground in the cytoplasm, which keeps the cytoplasmic potential constant relative to the external solution during vacuolar voltage clamping. Thus, the G_v can be measured in electrical isolation from the contribution of the plasma membrane. Root hairs offer easy physical access for the required dual impalements.

Lew (1996) reported an average root hair plasma membrane conductance of about 172 nS. For hair dimensions of about 8 by 90 μm, and epidermal cell component dimensions of 12.5 by 87.5 μm, the estimated specific conductance is about 2.9×10^{-3} S cm^{-2} (a specific resistance of 0.4 kΩ cm^2). The estimated conductance is expected to be higher than the real value because of the cable properties of the root hair (Meharg et al., 1994) and current leakage into adjacent cells (Lew, 1994, 1996). Cable properties and plasmodesmatal connections do not affect measurements of the G_v, 589 nS, yielding a specific conductance of 1.6×10^{-2} S cm^{-2} (a specific resistance of 0.062 kΩ cm^2). There is limited data available for G_v in higher plants. Holdaway-Clarke et al. (1996) reported an estimate of 1.45×10^{-4} S cm^{-2} in corn (*Zea mays*) suspension cells, almost equal to the plasma membrane conductance of 1.54×10^{-4} S cm^{-2}. In coenocytic algae (Characeae), Tester et al. (1987) compiled reported G_v from numerous sources. The majority of the reported values are in the range of 1 to

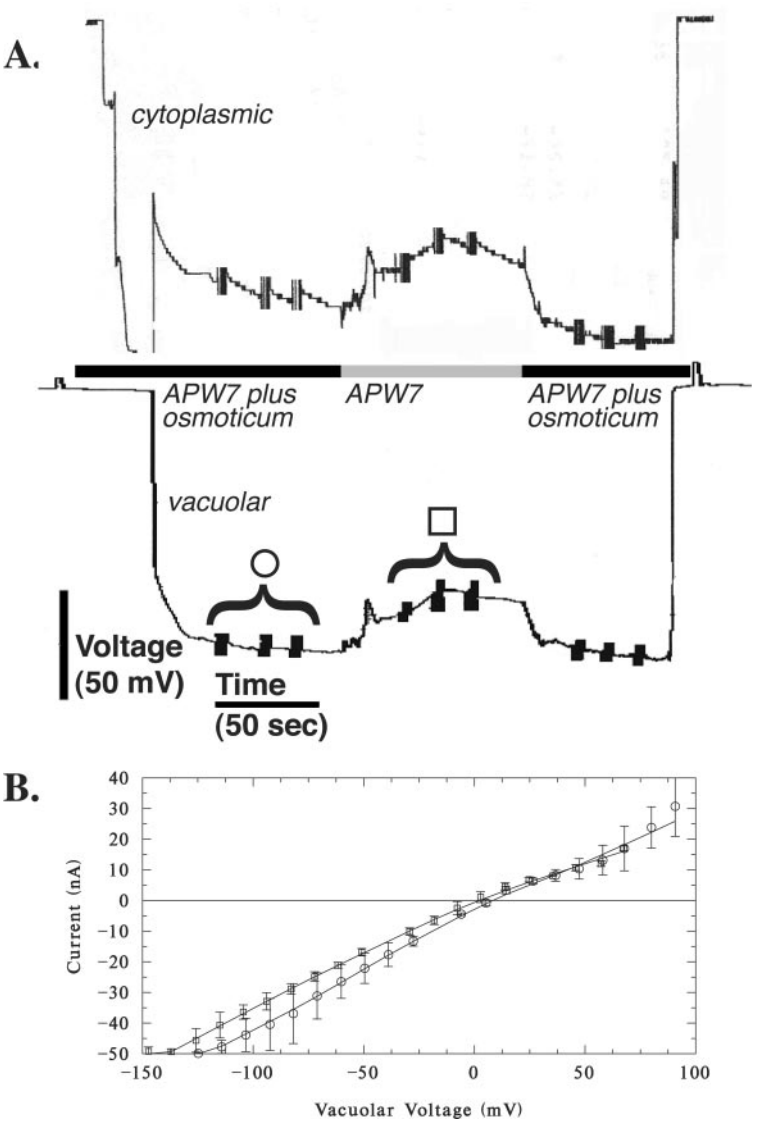

Figure 7. Vacuolar current-voltage relations: hypo-osmotic effect. A, An example of potential measurements from the cytoplasm and vacuole. Vertical bars on the potential traces show when voltage clamping was performed to obtain the current-voltage relation. B, Current-voltage measurements before (circles) and after (squares) hypo-osmotic treatment. The data are mean ± SD of three measurements, as shown in A. The current-voltage relations are linear in this example (with slight current activation at negative voltages). In other experiments, currents exhibited voltage activation at positive and negative voltage (five of nine experiments), or only at negative voltages (two of nine experiments). There was no systematic relation between the shape of the current-voltage curves and treatment (before and after).

2×10^{-2} S cm^{-2}, very similar to the Arabidopsis G_v reported here. The G_v is significantly higher that the plasma membrane conductance, indicative of large ion fluxes between the vacuole and the cytoplasm.

The voltage dependence of the current-voltage relations varied: Most current-voltage curves exhibited voltage-activated currents at negative and positive voltage, some were linear, and a few exhibited voltage-activated currents only at negative voltages. The differences were not related systematically to pretreatment or treatment conditions, and may reflect variable contributions of vacuolar ion channels (Barkla and Pantoja, 1996) to the overall conductance. It is possible that the properties of these (and other) ion channels, studied in vitro, are different under the completely physiological conditions used in the present experiments.

The relative contribution of the major osmotically active ions, K^+ and Cl^-, to the G_v can be estimated. Assuming K^+ and Cl^- are the major contributors to the G_v, the E_v will depend upon the relative vacuolar and cytoplasmic concentrations and the relative contribution of K^+ and Cl^- to membrane permeability, P_{Cl}/P_K:

$$E_v = 58 \times \log([K^+]_{cyt} + P_{Cl}/P_K \times [Cl^-]_{vac})/([K^+]_{vac} + P_{Cl}/P_K \times [Cl^-]_{cyt})$$

Using average concentrations from the data compiled by Luttge and Higinbotham (1979) and the measured E_v, the P_{Cl}/P_K is approximately 5.3, a value very similar to the ratio of the Characean algal vacuole in situ (7.1; Shimmen and Nishikawa, 1988).

In the context of hyperosmotic shock, the immediate response is a shift in net ion fluxes at the plasma membrane to counteract turgor loss. When using APW7 with 100 mM mannitol and 100 mM sorbitol to increase the osmolarity, turgor declines from 0.65 to 0.25 MPa; uptake of K^+, Cl^-, and Na^+ accounts for

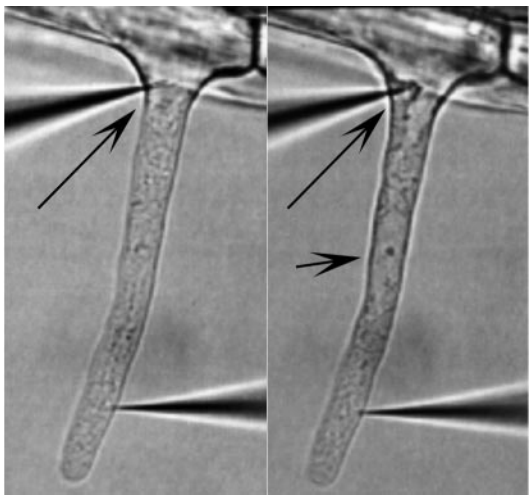

Figure 8. Example of cytoplasmic occlusion of vacuolar impalement. At the beginning of the experiment, the vacuolar micropipette (long arrow) appeared to be in the vacuole, but within 3 to 4 min, cytoplasm had "crept" around the tip (right), indicating that the tip location was cytoplasmic. This was confirmed by voltage clamp measurements, which indicated that the two double-barrel micropipettes were located in the same cellular compartment, the cytoplasm (data not shown). Note that the nucleus (short arrow) has migrated into the hair at this stage in root hair development. For scale, the root hair is about 8 μm in diameter.

turgor recovery over a period of about 30 min (Shabala and Lew, 2002). The hyperpolarization and decreased conductance at the plasma membrane are explained as an increase in the proton electrochemical gradient to "drive" ion uptake, and a decline in ion leakage from the root cells, respectively (Shabala and Lew, 2002). Because the vacuolar volume dominates the cell, even in the cytoplasm-rich root hair, the large increase in G_v would equilibrate cytoplasmic and vacuolar ion concentrations. The increased G_v occurs at negative and positive voltages (Fig. 4), and should reflect contributions from all major osmotically active ion species in the vacuole and cytoplasm. This may involve activation of K^+ and Cl^- channels in the tonoplast, or could be due to pressure/osmogradient activation of nonselective ion channels. Alexandre and Lassalles (1991) identified a 20-pS channel (P_K/P_{Cl} of approximately 3) that is activated by hydrostatic and osmotic pressure gradients. In whole vacuole voltage clamp in vitro, the pressure and osmotic gradient induced vacuolar currents exhibited voltage activation, mostly at positive voltages (Alexandre and Lassalles, 1991).

The results for hypo-osmotic stress are quite different. To minimize turgor increases caused by hypo-osmotic conditions, ion efflux from the cell would offer immediate relief, but this is not reflected in the behavior of the G_v, which remains unchanged.

Neither stress affects the resting potential of the vacuole. This implies that active electrogenic processes remain in equilibrium, and that the vacuole proton pumps, the V-ATPase and PP-ase (Maeshima, 2001), are not regulated by osmotic stresses in situ. Alternatively, changes in vacuolar proton pump activities may not affect the vacuolar potential due to counterion movement.

To summarize, in situ measurements of the vacuolar current-voltage relations reveal a rapid conductance increase in response to hyperosmotic stress. Hypo-osmotic stress has no effect. These responses are separate and distinct from changes in plasma membrane electrical properties (this paper and Lew, 1996). The results serve to highlight the real and immediate role of the vacuole in osmotic stress responses, well before significant changes in gene expression can take place.

MATERIALS AND METHODS

Seedling Preparation

Seeds of Arabidopsis (ecotype Columbia wild type) were surface sterilized with 0.5% (w/v) NaOCl, and sown on 0.8% (w/v) gellan gum (ICN Pharmaceuticals, Costa Mesa, CA) in modified APW5 (1 mM concentrations of KCl, $CaCl_2$, and $MgCl_2$, 2 mM Na_2SO_4, and 10 mM MES, pH adjusted to 5.0 with NaOH) in tissue culture dishes, and were incubated at room temperature (20°C–25°C under fluorescent lights [350–400 lux]). The plates were oriented vertically so that the roots grew down along the surface of the gellan gum. After 4 to 8 d, APW7 (0.1 mM KC1, 0.1 mM $CaCl_2$, 0.1 mM $MgCl_2$, 0.5 mM NaCl, and 1.0 mM MOPS, pH adjusted to 7.0 with NaOH) or APW7 plus osmoticum (50 mM mannitol and 50 mM sorbitol) was added to the culture dishes and impalements were begun after 1 to 3 h. Root hairs were accessible for impalement without having to disturb the roots, thus avoiding wounding responses. The hairs were observed every few minutes to ensure that they were elongating (Lew, 1991); growth rates were about 1 μm min^{-1}. The root hairs were impaled when they had attained a length of 80 to 100 μm. At this stage, the nuclei had migrated into the hair from the epidermal component of the root hair.

Micropipette Fabrication

Double-barreled micropipettes were constructed by placing two borosilicate (KG-33) capillaries with internal filaments (1 mm OD, 0.58 mm ID; Friedrich and Dimmock, Millville, NJ) within a nichromium heating filament, heating, and then twisting them 360°. The capillaries were then pulled on a vertical pipette puller (model P-30; Sutter, San Rafael, CA). The micropipettes were filled with 3 M KC1. Diffusion of KC1 into the cell should not affect the electrical properties of the cell because even ionophoretic injections of about 200 nC of K^+ or $C1^-$ are without effect on the membrane potential or current-voltage relations of the cell (data not shown).

Electrophysiology

The micropipette barrels were connected by AgCl electrodes to IE-251 electrometers (input impedance 10^{11} Ω; Warner Instruments, Hamden, CT), and to IE-201 and Duo 773 electrometers (input impedances 10^{11} Ω; Warner Instruments, Hamden, CT, and World Precision Instruments, Sarasota, FL, respectively). After placement in APW7, the electrodes were tested for crosstalk by injecting 1 nA of current through one electrode and checking for significant voltage deflections in the other electrode of each double-barrel micropipette; crosstalk was zero to minimal (<5%). Grounding was via a 2-mm capillary containing 3 M KC1 (to match the micropipette KC1 concentration) in 2% (w/v) agar connected to an AgCl electrode.

Microscopy

An upright microscope (Optiphot; Nikon Canada, Mississauga, Ontario) was used with a ×40 water immersion objective (NA 0.75) under bright-field conditions. After impalement, the image was often recorded on a CCD

video camera (model KP-M1; Hitachi Denshi, Tokyo) and printed on a video printer (Mitsubishi Electronics America, Somerset, NJ).

Voltage Clamping

Current-voltage measurements using a voltage clamp (Smith et al., 1980) have been described previously (Lew, 1991). Voltage clamping for current-voltage measurements was computer driven through a data acquisition board (Scientific Solutions, Mentor, OH) and operational amplifier configured for voltage clamping. Because the vacuolar current-voltage properties were being measured, it was necessary to configure the other double-barrel micropipette as a virtual ground (Fig. 3B). With the tip located in the cytoplasm, this held the cytoplasmic voltage constant at the resting potential while current-voltage measurements of the vacuole were being performed. In control experiments, long-term (4–8 min) voltage clamp of the cytoplasm at the resting potential did not affect the root hair (data not shown).

A bipolar staircase (alternating positive and negative clamps) of 100 ms voltage clamps followed by a voltage clamp at the resting potential minimized any possible hysteresis effects. Data sampling (voltage and current) was performed during the last 10 ms of the voltage clamp.

Vacuolar ion channels measured in vitro are characterized as fast or slow (Barkla and Pantoja, 1996) with low cation selectivity. Reported time dependence of the slow vacuolar channel is in the range of 300 to 500 ms for half-maximal activation, and 1 to 2 s for complete activation (Allen and Sanders, 1995; Ward et al., 1995). Assuming the time dependence is the same in situ, the current-voltage measurements are selecting for fast vacuolar ion channels.

To determine the G_v, linear regression was used. This effectively averages any changes, voltage-activated or inactivated currents, in the current-voltage relations. These were observed in some but not all experiments, as noted in "Results."

Cytoplasmic and Vacuolar Impalements

One double-barrel micropipette was impaled into the cytoplasmic, typically within 20 μm of the root hair tip, where the root hair is cytoplasm rich, with no central vacuole. The other double-barrel micropipette was impaled into the vacuole at the region where the root hair emerges from the epidermal part of the root hair cell (Fig. 1). The location of the cytoplasm impalement in the cytoplasm was confirmed using fluorescent dye injections, as were vacuolar impalements (Lew, 2000). However, the vacuolar impalement was more difficult to execute successfully. Confirmation of the vacuolar location of the double-barrel micropipette after impalement relied upon the fidelity of the voltage clamping. If both double-barrel micropipettes were located in the cytoplasm, the virtual ground circuit effectively cancelled any attempt to voltage clamp. This was common, even when the double-barrel micropipette was visually impaled into the vacuole. The likely interpretation is that the vacuole membrane was wrapped around the double-barrel micropipette tip, effectively excluding it from the vacuole compartment. In some cases, active exclusion was observed as cytoplasm crept up the micropipette tip, eventually surrounding it (Fig. 8).

Statistical Analysis

All data are shown as mean ± SD (sample size) unless otherwise noted. Statistical analyses were performed in Systat (Systat, Evanston, IL).

ACKNOWLEDGMENTS

Special thanks to the anonymous reviewers for their comments and thoughtful suggestions.

Received August 6, 2003; returned for revision September 4, 2003; accepted September 22, 2003.

LITERATURE CITED

Alexandre J, Lassalles J-P (1990) Effect of D-*myo*-inositol 1, 4, 5-triphosphate on the electrical properties of the red beet vacuolar membrane. Plant Physiol **93:** 837–840

Alexandre J, Lassalles J-P (1991) Hydrostatic and osmotic pressure activated channels in plant vacuole. Biophys J **60:** 1326–1336

Allen GJ, Sanders D (1995) Calcineurin, a type 2B protein phosphatase, modulates the Ca^{2+}-permeable slow vacuolar ion channel of stomatal guard cells. Plant Cell **7:** 1473–1483

Barkla BJ, Pantoja O (1996) Physiology of ion transport across the tonoplast of higher plants. Annu Rev Plant Physiol Plant Mol Biol **47:** 159–184

Berecki G, Eijken M, Van Iren F, Van Duijn B (2001) Tonoplast anion channel activity modulation by pH in *Chara corralina.* J Membr Biol **184:** 131–141

Bethke PC, Jones RL (1994) Ca^{2+}-calmodulin modulates ion channel activity in storage protein vacuoles of barley aleurone cells. Plant Cell **6:** 277–285

Bouteau F, Pennarun A-M, Kurkdjian A, Convert M, Cornel D, Monestiez M, Rona J-P, Bousquet U (1999) Ion channels of intact young root hairs from *Medicago sativa.* Plant Physiol Biochem **37:** 889–898

Bruggemann LI, Pottosin II, Schonknecht G (1998) Cytoplasmic polyamines block the fast-activating vacuolar cation channel. Plant J **16:** 101–105

Carpaneto A, Cantu AM, Gambale F (1999) Redox agents regulate ion channel activity in vacuoles from higher plant cells. FEBS Lett **442:** 129–132

Carpaneto A, Cantu AM, Gambale F (2001) Effects of cytoplasmic Mg^{2+} on slowly activating channels in isolated vacuoles of *Beta vulgaris.* Planta **213:** 457–468

Covic L, Silva NF, Lew RR (1999) Functional characterization of ARAKIN (ATMEKK1): a possible mediator in an osmotic stress response pathway in higher plants. Biochim Biophys Acta **1451:** 242–254

Cuin TA, Miller AJ, Laurie SA, Leigh RA (2003) Potassium activities in cell compartments of salt-grown barley leaves. J Exp Bot **54:** 657–661

Dobrovinskaya OR, Muniz J, Pottosin II (1999) Inhibition of vacuolar ion channels by polyamines. J Membr Biol **167:** 127–140

Felle H (1994) The H^+/Cl^- symporter in root-hair cells of *Sinapis alba.* Plant Physiol **106:** 1131–1136

Gong XQ, Bisson MA (2002) Acetylcholine-activated Cl^- channel in the *Chara* tonoplast. J Membr Biol **188:** 107–113

Hasegawa PM, Bressan RA, Zhu JK, Bohnert HJ (2000) Plant cellular and molecular responses to high salinity. Annu Rev Plant Physiol Plant Mol Biol **51:** 463–499

Hedrich R, Neher E (1987) Cytoplasmic calcium regulates voltage-dependent ion channels in plant vacuoles. Nature **329:** 833–836

Heidecker M, Wegner LH, Binder K-A, Zimmerman U (2003) Turgor pressure changes trigger characteristic changes in the electrical conductance of the tonoplast and the plasmalemma of the marine alga *Valonia utriculatus.* Plant Cell Environ **26:** 1035–1051

Holdaway-Clarke TL, Walker NA, Overall RL (1996) Measurement of the electrical resistance of plasmodesmata and membranes of corn suspension-culture cells. Planta **199:** 537–544

Horowitz P, Hill W (1989) The Art of Electronics. Cambridge University Press, Cambridge, UK

Ivashikina N, Becker D, Ache P, Meyerhoff O, Felle HH, Hedrich R (2001) K^+ channel profile and electrical properties of *Arabidopsis* root hairs. FEBS Lett **508:** 463–469

Lew RR (1991) Electrogenic transport properties of growing *Arabidopsis* root hairs: the plasma membrane proton pump and potassium channels. Plant Physiol **97:** 1527–1534

Lew RR (1994) Regulation of electrical coupling between *Arabidopsis* root hairs. Planta **193:** 67–73

Lew RR (1996) Pressure regulation of the electrical properties of growing *Arabidopsis thaliana* root hairs. Plant Physiol **112:** 1089–1100

Lew RR (2000) Electrobiology of root hairs. *In* RW Ridge, AM Emons, eds, Cell and Molecular Biology of Root Hairs. Springer-Verlag, Tokyo, pp 115–139

Luttge U, Higinbotham N (1979) Transport in Plants. Springer-Verlag, New York

Maeshima M (2001) Tonoplast transporters: organization and function. Annu Rev Plant Physiol Plant Mol Biol **52:** 469–497

Martinoia E, Massonneau A, Frangne N (2000) Transport processes of solutes across the vacuolar membrane of higher plants. Plant Cell Physiol **41:** 1175–1186

Matile P (1978) Biochemistry and function of vacuoles. Annu Rev Plant Physiol **29:** 193–213

Meharg AA, Mauroussset L, Blatt MR (1994) Cable correction of membrane currents recorded from root hairs of *Arabidopsis thaliana* L. J Exp Bot **45:** 1–6

Meijer HGJ, Munnik T (2003) Phospholipid-based signaling in plants. Annu Rev Plant Physiol Plant Mol Biol **54:** 265–306

Miller AJ, Cookson SJ, Smith SJ, Wells DM (2001) The use of microelectrodes to investigate compartmentation and the transport of metabolized inorganic ions in plants. J Exp Bot **52:** 541–549

Ober ES, Sharp RE (2003) Electrophysiological responses to maize roots to low water potentials: relationship to growth and ABA accumulation. J Exp Bot **54:** 813–824

Pei ZM, Ward JM, Harper JF, Schroeder JI (1996) A novel chloride channel in *Vicia faba* guard cell vacuoles activated by the serine/threonine kinase, CDPK. EMBO J **15:** 6564–6574

Pei ZM, Ward JM, Shroeder JI (1999) Magnesium sensitizes slow vacuolar channels to physiological cytosolic calcium and inhibits fast vacuolar channels in fava bean guard cell vacuoles. Plant Physiol **121:** 977–986

Pottosin II, Martinez-Estevez M (2003) Regulation of the fast vacuolar channel by cytosolic and vacuolar potassium. Biophys J **84:** 977–986

Reifarth FW, Weiser T, Bentrup FW (1994) Voltage- and Ca^{2+}-dependence of the K^+ channel in the vacuolar membrane of *Chenopodium rubrum* L. suspension cells. Biochim Biophys Acta **1192:** 79–87

Schulz-Lessdorf B, Dietrich P, Marten I, Lohse G, Busch H, Hedrich R (1994) Coordination of plasma membrane and vacuolar membrane ion channels during stomatal movement. Symp Soc Exp Biol **48:** 99–112

Shabala SN, Lew RR (2002) Turgor regulation in osmotically stressed *Arabidopsis* epidermal root cells: direct support for the role of inorganic ion uptake as revealed by concurrent flux and cell turgor measurements. Plant Physiol **129:** 290–299

Shimmen T, Nishikawa S (1988) Studies on the tonoplast action potential of *Nitella flexilis*. J Membr Biol **101:** 133–140

Smith TG Jr, Barker JL, Smith BM, Colburn TR (1980) Voltage clamping with microelectrodes. J Neurosci Methods **3:** 105–128

Tester M, Beilby MJ, Shimmen T (1987) Electrical characteristics of the tonoplast of *Chara corallina*: a study using permeabilized cells. Plant Cell Physiol **28:** 1555–1568

Tyerman SD, Bohnert HJ, Maurel C, Steudle E, Smith JAC (1999) Plant aquaporins: their molecular biology, biophysics and significance for plant water relations. J Exp Bot **50:** 1055–1071

van den Wijngaard PW, Bunney TD, Roobeek I, Schonknecht G, de Boer AH (2001) Slow vacuolar channels from barley mesophyll cells are regulated by 14-3-3 proteins. FEBS Lett **488:** 100–104

Walker DJ, Leigh RA, Miller AJ (1996) Potassium homeostasis in vacuolate plant cells. Proc Natl Acad Sci USA **93:**10510–10514

Ward JM, Pei Z-M, Schroeder JI (1995) Roles of ion channels in initiation of signal transduction in higher plants. Plant Cell **7:** 833–844

Ward JM, Schroeder JI (1994) Calcium-activated K^+ channels and calcium-induced calcium release by slow vacuolar ion channels in guard cell vacuoles implicated in the control of stomatal closure. Plant Cell **6:** 669–683

White PJ (2000) Calcium channels in higher plants. Biochim Biophys Acta **1465:** 171–189

Zhu JK (2002) Salt and drought stress signal transduction in plants. Annu Rev Plant Physiol Plant Mol Biol **53:** 247–273